

Microstructure and Mechanical Properties of Rolled and Annealed Mg-Y-Zr-xNd Alloys

Dai Yan¹, Chen Xianhua^{1,2}, Xu Xiaoyang¹, Zhao Chaoyue¹, Liu Chunquan¹,
Zhao Di¹, Liu Xiaofang¹, Luo Zhu¹, Tu Teng¹, Pan Fusheng^{1,2}

¹ International Joint Laboratory for Light Alloys (Ministry of Education), Chongqing University, Chongqing 400044, China; ² Chongqing Academy of Science and Technology, Chongqing 401123, China

Abstract: Microstructures and mechanical properties of Mg-5Y-0.6Zr-xNd ($x=0, 0.5$ and $1\text{wt}\%$) alloys under various heat treatment conditions were investigated by optical microstructure (OM), scanning electron microscope (SEM), X-ray diffraction (XRD), electron backscatter diffraction (EBSD) and tensile tests. The results show that with the increase Nd of content, the amount of second phases Mg_{24}Y_5 and $\text{Mg}_{14}\text{Nd}_2\text{Y}$ (β) increases in the matrix. Minor Nd addition can reduce the stacking fault energy of α -Mg and promote the dynamic recrystallization during hot-rolled process. As the Nd content increases, the volume fraction of static recrystallization is promoted obviously. The average grain size of Mg-5Y-0.6Zr-0Nd alloy after annealing treatment can be refined to $3.73\ \mu\text{m}$. Tensile strength of as-rolled alloys increases with the addition of Nd, while the elongation decreases. As-rolled alloy sheet with $1.01\ \text{wt}\%$ Nd exhibits remarkable mechanical properties, in which the values of ultimate tensile strength, yield strength and elongation are $336\ \text{MPa}$, $278\ \text{MPa}$ and 16.3% , respectively. Based on the microstructure observation, the changes of mechanical properties were discussed.

Key words: Mg-Y-Zr-Nd alloys; microstructure; mechanical properties; recrystallization

With the rapid development of technology, magnesium alloys have attracted tremendous research in the last few decades. As the lightest structural metal material, Mg alloys are increasingly used in aerospace, automotive and 3C industries^[1-5]. However, the relatively poor mechanical properties, low ductility and low high temperature creep-resistant restrict the widespread uses of Mg alloys^[6-8]. The low mechanical properties of Mg alloys are due to the hexagonal closely packed (hcp) crystal structure, which results in a lack of operational slip systems^[9,10]. This greatly reduces the workability of Mg alloys, which is one of the major problems that hinder its widespread application^[11,12]. Therefore, it takes great efforts to improve the strength, and element alloying is one of the important methods^[13,14].

Alloying is an effective method to improve the mechanical properties of Mg alloys. Thermomechanical processes can im-

prove the formability of Mg through grain refinement. As-rolled Mg alloys with higher mechanical strength are expected to get more applications compared with the cast alloy^[15]. Since the last century, rare earth metals (RE) have been used to improve the mechanical properties of Mg alloys, particularly at elevated temperatures^[16-18]. Due to its high strength and creep resistance, the WE (Mg-Y-RE) series has been successfully used in aerospace and automotive applications. Based on WE series, two commercially available alloys have been successfully developed, WE43 (Mg-4.0% Y-3.3% RE-0.5%Zr) and WE54 (Mg-5.1%-Y-3.3%RE-0.5%Zr)^[19]. The tensile strength, yield strength and elongation of WE43 alloy are $250\ \text{MPa}$, $165\ \text{MPa}$ and 2% , respectively^[20]. There are three main precipitates of WE series alloy, namely metastable phase β'' , intermediate phase β' and equilibrium phase β ($\text{Mg}_{14}\text{Nd}_2\text{Y}$). It is suggested that these pre-

Received date: July 25, 2018

Foundation item: National Key R&D Program of China (2016YFB0301100); National Natural Science Foundation of China (51571043, 51531002); Fundamental Research Funds for the Central Universities (2018CDJDCL0019, cqu2018CDHB1A08)

Corresponding author: Chen Xianhua, Ph. D., Professor, College of Materials Science and Engineering, Chongqing University, Chongqing 400045, P. R. China, Tel: 0086-23-65102633, E-mail: xhchen@cqu.edu.cn

Copyright © 2019, Northwest Institute for Nonferrous Metal Research. Published by Science Press. All rights reserved.

cipitates play an indispensable role in strengthening such Mg alloys. And another element Zr, as the currently most effective grain refiner, also can improve the strength of Mg alloys. Wang et al.^[21] studied the hot-rolled Mg-4Y-2.5Nd-0.6Zr alloy and obtained tensile strength, yield strength and elongation of 290 MPa, 235 MPa, and 10%, respectively. The tensile strength, yield strength and elongation of Mg-3.5Y-2.5Nd-0.5Zr alloy obtained after solution treatment at 798 K for 4 h and subsequent aging at 498 K for 34 h by Li et al.^[22] were 301 MPa, 202 MPa and 6.9%, respectively.

However, there were few studies in detail on the use of element alloying to improve the mechanical properties of WE series alloys. In this work, three Mg-Y-Zr-Nd alloys with different Nd were prepared. It is aimed to improve the ultimate tensile strength, yield strength and elongation of Mg-Y-Nd-Zr alloys through adjusting the alloy elements Nd content and different annealing processes and then to illustrate the changes of microstructure and mechanical properties in hot-rolled Mg-Y-Zr-Nd alloy after the addition of Nd.

1 Experiment

Experimental magnesium alloys were prepared from commercial high-purity Mg (99.98 wt%), Mg-30wt%Y, Mg-30wt%Nd, and Mg-27.85wt%Zr master alloy were used as raw materials. Three alloy ingots with Nd content of 0, 0.5, 1 wt% were prepared through conventional casting under the mixed atmosphere of CO₂ and SF₆ (100:1). The actual chemical compositions of these alloys was determined by an inductively coupled plasma analyzer, as listed in Table 1. Alloys containing 0, 0.49% and 1.01%Nd were denoted YKN0, YKN0.5, and YKN1, respectively. The ingots were homogenized at 500 °C for 10 h. And then the sample was extruded at 400 °C with an extrusion ratio of 11.5:1. The cross-section of the extruded sheets was 8 mm × 125 mm. The as-extruded 8 mm thick Mg-Y-Zr-xNd alloy sheet was hot-rolled at 400 °C to the thickness of 3.3 mm. The total thickness reduction was about 60%, and the reduction per pass was 5%. The sheets were heat-treated at 400 °C between passes to stabilize the rolling temperature, and subsequently sheets were annealed at 200 °C for 1h and 400 °C for 20 min.

The constituent phases of the as-cast alloys were identified by X-ray diffraction (XRD, Rigaku D/MAX-2500PC). Microstructures were examined by optical microscopy (OM) and scanning electron microscopy (SEM, TESCAN VEGA II LMU). For OM and SEM observation, polished specimens were etched with a mixture of 0.8 g picric acid, 10 mL ethanol, 2 mL acetic acid and 2 mL water. The static microstructure of YKN0, YKN0.5, and YKN1 alloys were examined by electron back scattering diffraction (EBSD, FEI Nova 400 FEG equipped with an HKL channel 5 systems). The sample was prepared by mechanical grinding for EBSD orientation mapping and then electropolishing with a solution of 100 mL isopropanol + 800 mL ethanol + 18.5 mL distilled water + 10 g hydroxyquinoline + 75 g citric acid + 41.5 g sodium thiocyanate + 15 mL perchloric acid cooled to -30 °C at 20 V for 90 s.

Table 1 Chemical composition of Mg-Y-Zr-xNd alloys (wt%)

Alloy	Mg	Y	Nd	Zr
YKN0	Bal.	4.95	0	0.53
YKN0.5	Bal.	4.98	0.49	0.64
YKN1	Bal.	5.08	1.01	0.74

Tensile tests were conducted at room temperature by a CMT-5105 material testing machine with a strain rate of $1 \times 10^{-3} \text{ s}^{-1}$. The hot-rolled and subsequently annealed sheets were cut into rectangular tensile specimens with a gage length of 25 mm and cross-sectional area of 2 mm × 5 mm by an electrical sparking wire cutting machine. Three tensile samples were used for each alloy. Tensile direction was parallel to the rolling direction. The tensile fracture surfaces of the investigated alloys were observed by SEM backscattered electron imaging.

2 Results and Discussion

2.1 Microstructure

The XRD patterns of Mg-Y-Zr-xNd alloys annealed at 200 °C for 1 h are shown in Fig.1. With partially magnified images at the top left of the curve. The phase composition of the alloy by XRD analysis presents that they are mainly composed of α -Mg and Mg₂₄Y₅ phase, and β (Mg₁₄Nd₂Y) phase appears when the Nd content is 1.01%. The quantity and composition of second phase change with the increase of Nd content. With the increase of Nd content, the amount of β and Mg₂₄Y₅ phases are gradually increased. It can be concluded that increasing Nd content can reduce the solid solubility of Y atom in Mg matrix and make more Y atoms precipitate in the form of intermetallic compounds^[23,24]. When the Nd content is 1.01%, Nd-containing ternary phase β begins to appear in the alloy, which has similar crystal structure and diffraction characteristics to Mg₅Gd^[25].

Optical micrographs (OM) of hot-rolled alloys are presented in Fig.2. As can be seen from Fig.2a, the microstructure of as-rolled YKN0 alloy consists of coarse grains and a small amount of dynamic recrystallization (DRX) grains. The size of coarse and fine grains is about 8 and 3 μm , respectively. It is not

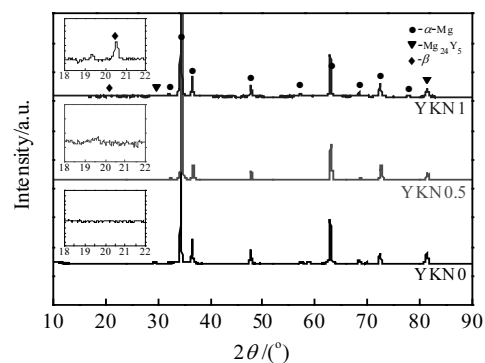


Fig.1 XRD patterns of Mg-Y-Zr-xNd alloy annealed at 200 °C/1 h

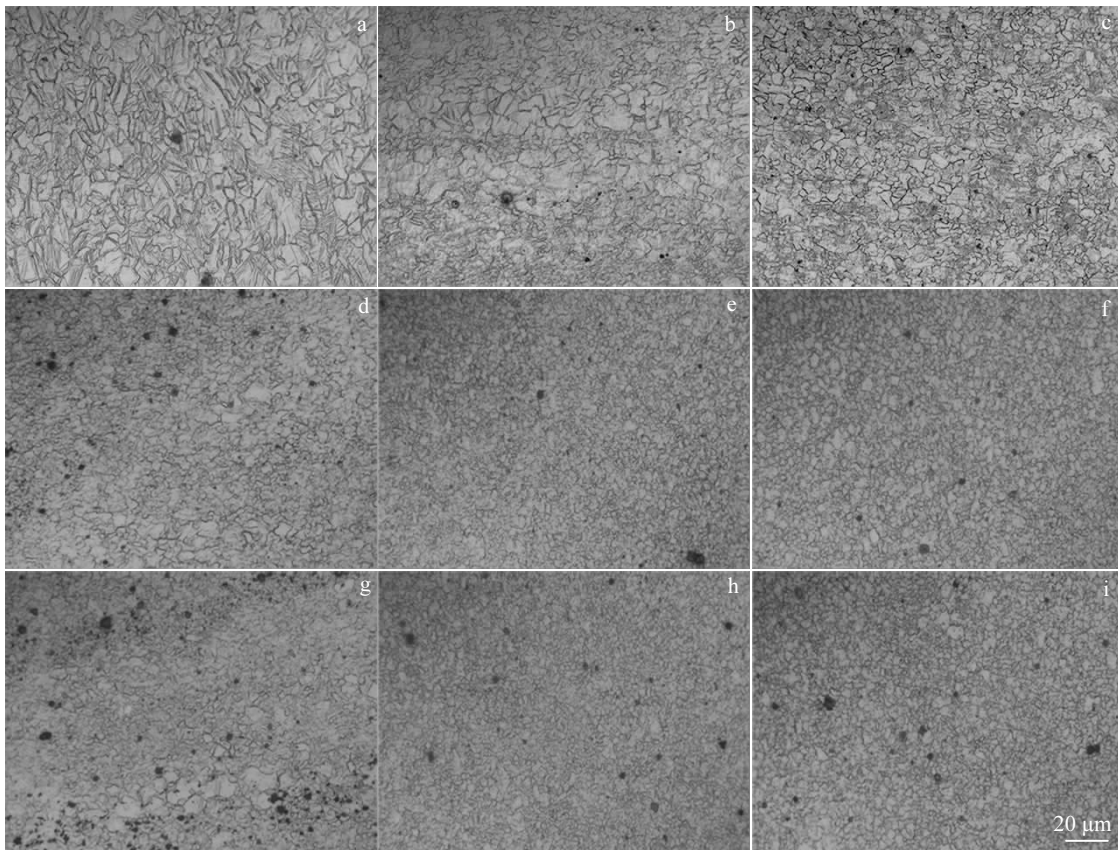


Fig.2 OM microstructure of rolled and annealed sheets: (a) as-rolled YKN0; (b) YKN0 annealed at 200 °C/1 h; (c) YKN0 annealed at 400 °C/20 min; (d) as-rolled YKN0.5; (e) YKN0.5 annealed at 200 °C/1 h; (f) YKN0.5 annealed at 400 °C/20 min; (g) as-rolled YKN1; (h) YKN1 annealed at 200 °C/1 h; (i) YKN1 annealed at 400 °C/20 min

difficult to find the presence of twins in coarse grains. After addition of Nd (Fig.2d and 2g), the fraction of DRX grains increase and almost no twins are observed. This indicates that the addition of Nd can help to refine the alloy microstructure. It is obvious that Nd element plays a crucial role in promoting DRX and affects grain size. On the one hand, Nd is one of the effective alloying elements to reduce the stacking fault energy of α -Mg matrix^[26,27]. The lower the stacking fault energy, the wider the extended dislocation, thus dislocation constriction and cross slip of the extended dislocation become more difficult^[28]. The resulting high-density dislocations and high deformed energy storage are one of factors leading to DRX. On the other hand, the $Mg_{24}Y_5$ phase particles can act as nucleation sites and promote DRX during hot-rolling, i.e. particle stimulate nucleation (PSN) of recrystallization. $Mg_{24}Y_5$ phase can also promote DRX by piling up dislocations, which increases the strain energy and acts as the driving force for DRX^[29,30].

As can be seen, from Fig.2b, 2e, 2h and Fig.2c, 2f, 2i, the alloys have the equiaxed structure with the average grain size about 3 μm . Grain refinement is obvious with the increase of Nd content. On the one hand, the grains of Nd-containing alloys before rolling are smaller than that of the Nd-free alloy^[23].

On the other hand, increasing Nd content can reduce the number of Y atoms in α -Mg, and more $Mg_{24}Y_5$ and β phases are dispersed in the matrix, which can prevent the grain boundary movement and refine grains. In addition, there are some punctiform black second phases, and as the Nd content increases, the black second phases increase. According to XRD (Fig.1) and the EDS analysis (Fig.6h) results, it is demonstrated that the black second phases are $Mg_{24}Y_5$.

The microstructure tended to be equiaxed grain when the alloys were rolled and subsequently annealed. Fig.3 presents electron backscatter diffraction (EBSD) images of the as-rolled YKN0 alloy and the subsequently annealed alloy and their corresponding misorientation angle and grain size distribution of. The initial EBSD map in as-rolled microstructure shows some coarse grains with diameter of 15~20 μm and finer grains with diameter of 2~5 μm (Fig.3a). The twins decrease significantly after annealing at 200 °C for 1 h (Fig.3b). The small static recrystallization (SRX) grains become visible near the twins. As the annealing temperature reaches 400 °C and is held for 20min, full recrystallization is evident, and the average fine grain size decreases to 3.73 μm (Fig.3c). There are a lot of twins caused by the large hot deformation in

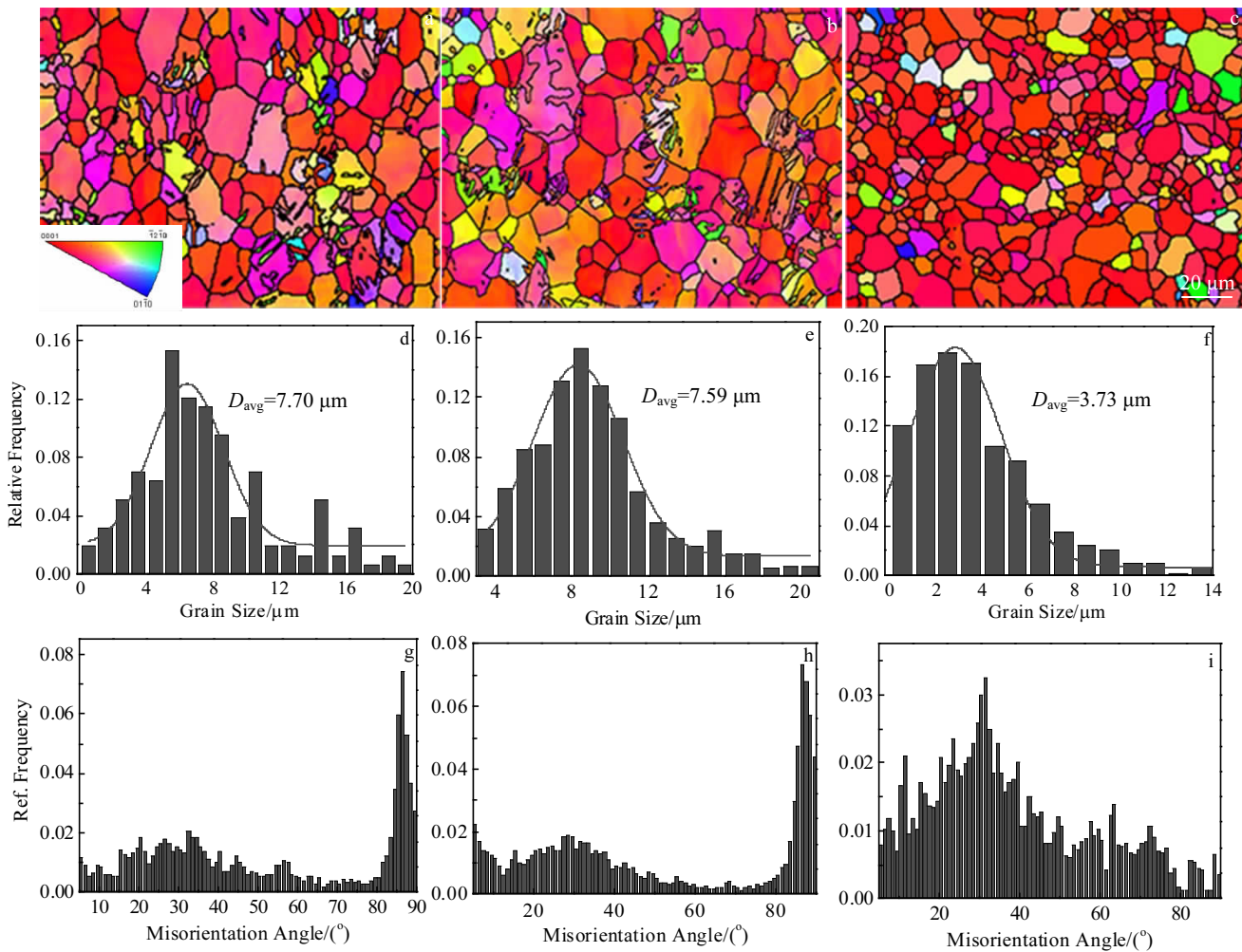


Fig.3 EBSD images (a~c) and corresponding relatively frequency and grain size distribution (d~f) and misorientation angle (g~i) of the investigated YKN0 alloys: (a, d, g) as-rolled, (b, e, h) annealed at 200 °C for 1 h, and (c, f, i) annealed at 400 °C for 20 min

Fig.3a, which has higher stored energies than that of the remainder of the material. The presence of twins with higher storage energy leads to the nucleation of recrystallization during annealing^[31,32]. It is why SRX grains can be seen to have been formed near the twins and accompanied by grain growth and no twins remain (Fig.3c). In addition, the misorientation angles are shown for the three kinds of alloys in Fig.3g~3h. In this work, only boundaries with misorientation angles $>5^\circ$ were considered. The prominent boundary misorientation is $85^\circ \sim 90^\circ$ in the Fig.3g and 3h, and Fig.3i is $25^\circ \sim 35^\circ$. The peak of $85^\circ \sim 90^\circ$ in the misorientation angle distribution is clearly attributable to a significant proportion of $\{11\bar{2}0\}$ twinning^[33]. The misorientation angle of $85^\circ \sim 90^\circ$ disappears after annealing 400 °C for 20 min (Fig.3i), which is caused by the full SRX.

The XRD pole figures of the samples in the as-rolled and annealed, respectively states and their two annealing systems are shown in Fig.4 and Fig.5. The as-rolled alloy exhibits a typical strong (0002) basal texture, and the annealed sheet is still the basal texture, and bimodal base texture is formed

along the TD direction. Texture strength after annealing is weakened compared with that before annealing, and the basal texture strength of the alloys under the same condition is also weakened with the increase of Nd content (Fig.5). The maximum pole intensity of the as-rolled alloys is reduced remarkably with the increase of Nd content due to the high-volume fraction of DRX grains, showing that the addition of Nd can effectively weaken the basal texture. DRX occurs in the alloys containing Nd and the grain size is finer through the mechanism of the $Mg_{24}Y_5$ phase PSN. At the same time, the orientation distributions of DRX grains are random, and thus weakening the recrystallization texture^[34,35]. Similarly, Nd-containing alloys decrease by $\sim 33\%$ in the texture of the two-state annealed compared to the Nd-free alloy (Fig.5). Annealing at 200 °C/1 h and 400 °C/20 min provide good conditions for recrystallization to impart the modifications observed in the annealing textures. In a word, the observed basal texture weakening in the present work upon hot-roll and annealing can be related to PSN of recrystallization.

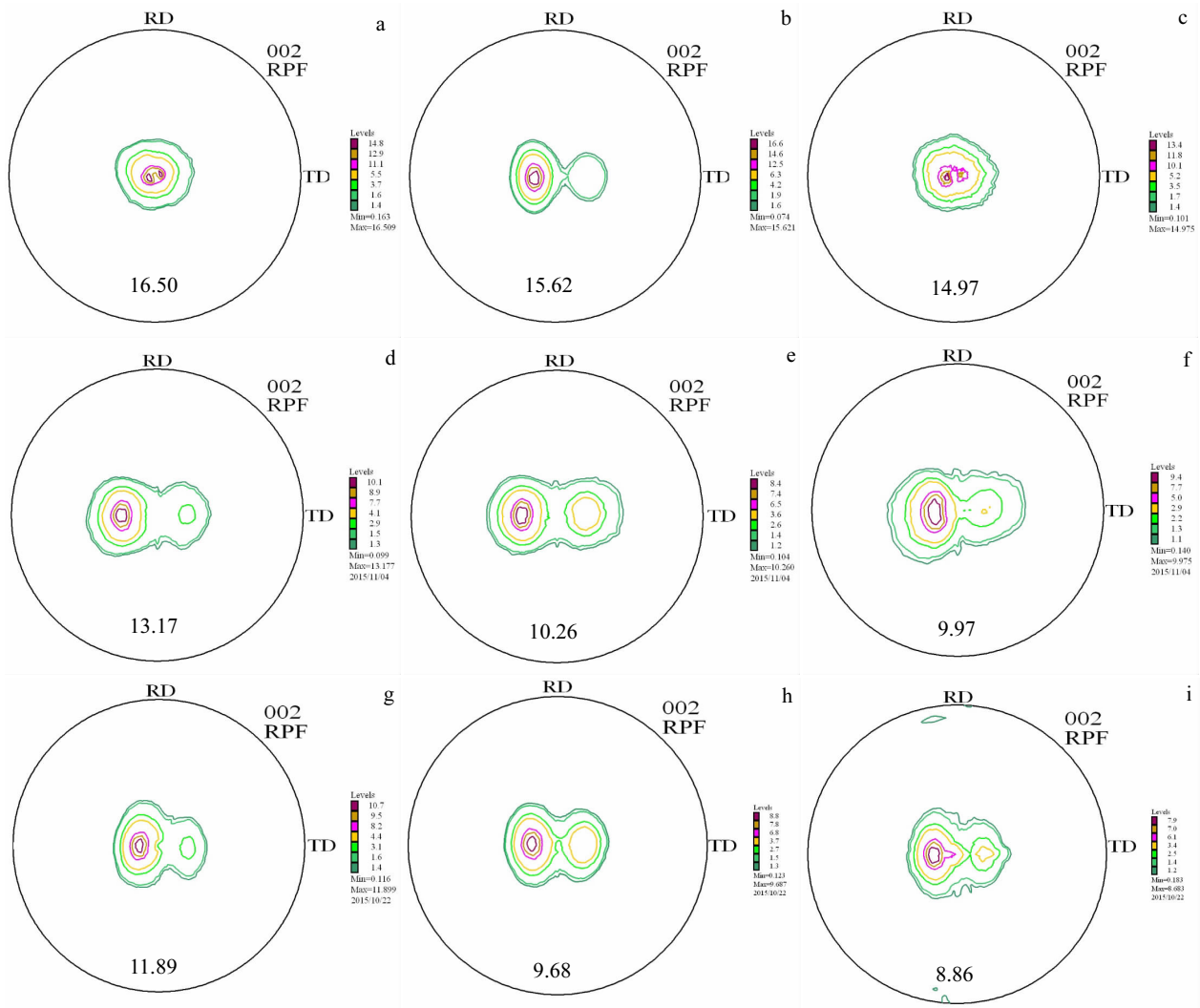


Fig.4 XRD pole figure of the rolled and annealed alloy sheets: (a) as-rolled YKN0; (b) YKN0 annealed at 200 °C/1 h; (c) YKN0 annealed at 400 °C/20 min; (d) as-rolled YKN0.5; (e) YKN0.5 annealed at 200 °C/1 h; (f) YKN0.5 annealed at 400 °C/20 min; (g) as-rolled YKN1; (h) YKN1 annealed at 200 °C/1 h; (i) YKN1 annealed at 400 °C/20 min

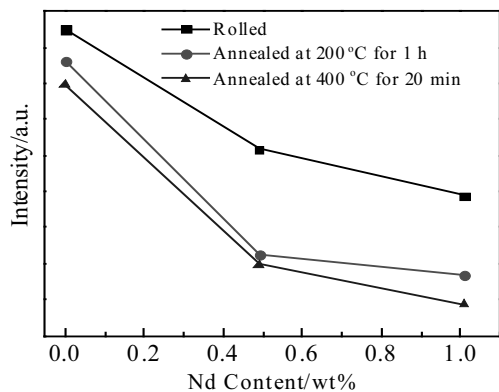


Fig.5 Effect of Nd content on basal texture intensity of different states

2.2 Tensile properties

The room temperature tensile properties of the Mg-Y-Zr-xNd alloys with different conditions are shown in Table 2. Minor Nd addition and annealing temperature have significant effects on tensile properties. The UTS of YKN0, YKN0.5 and YKN1 rolled sheets are 317, 326 and 336 MPa, respectively. The alloy with 1.01% Nd exhibits the maximum UTS and YS, and their values are 336 and 278 MPa, respectively. Compared with the alloy without Nd element, the UTS and YS increase by 19 MPa and 11 MPa, respectively. High strength and relatively lower elongation may be due to the work hardening caused by plastic deformation. In addition, the existence of a large number of twins also increases the strength of the alloy because the twin boundaries can increase the resistance to dislocation motion, and the smaller the twins, the higher the twin resistance is^[36,37].

Table 2 Tensile properties of rolled and annealed Mg-Y-Zr-xNd sheets

Alloy	UTS/MPa	YS/MPa	EL/%
YKN0 as-rolled	317	267	18.5
YKN0 annealed for 200 °C/1 h	302	253	21.0
YKN0 annealed for 400 °C/20 min	285	239	22.3
YKN0.5 as-rolled	326	233	17.4
YKN0.5 annealed for 200 °C/1 h	319	213	23.0
YKN0.5 annealed for 400 °C/20 min	308	204	21.0
YKN1 as-rolled	336	278	16.3
YKN1 annealed for 200 °C/1 h	317	267	20.3
YKN1 annealed for 400 °C/20 min	314	259	20.0

The excellent mechanical properties of the sheets of the as-rolled Mg-Y-Zr-xNd alloys can be attributed to the following reasons: Firstly, after annealing at 400 °C for 20 min, the grain size is greatly reduced from 7.70 μm for the as-rolled sample to 3.73 μm for the annealed sample. It illustrates that the grain size is obviously refined by SRX occurring during annealing and strain storage energy is released, which reduces dislocation density and softens of the alloy. According to the Hall-Petch relationship, the yield stress depends on the grain size and follows the principle:

$$\Delta\sigma_{GS}=Kd^{1/2} \quad (1)$$

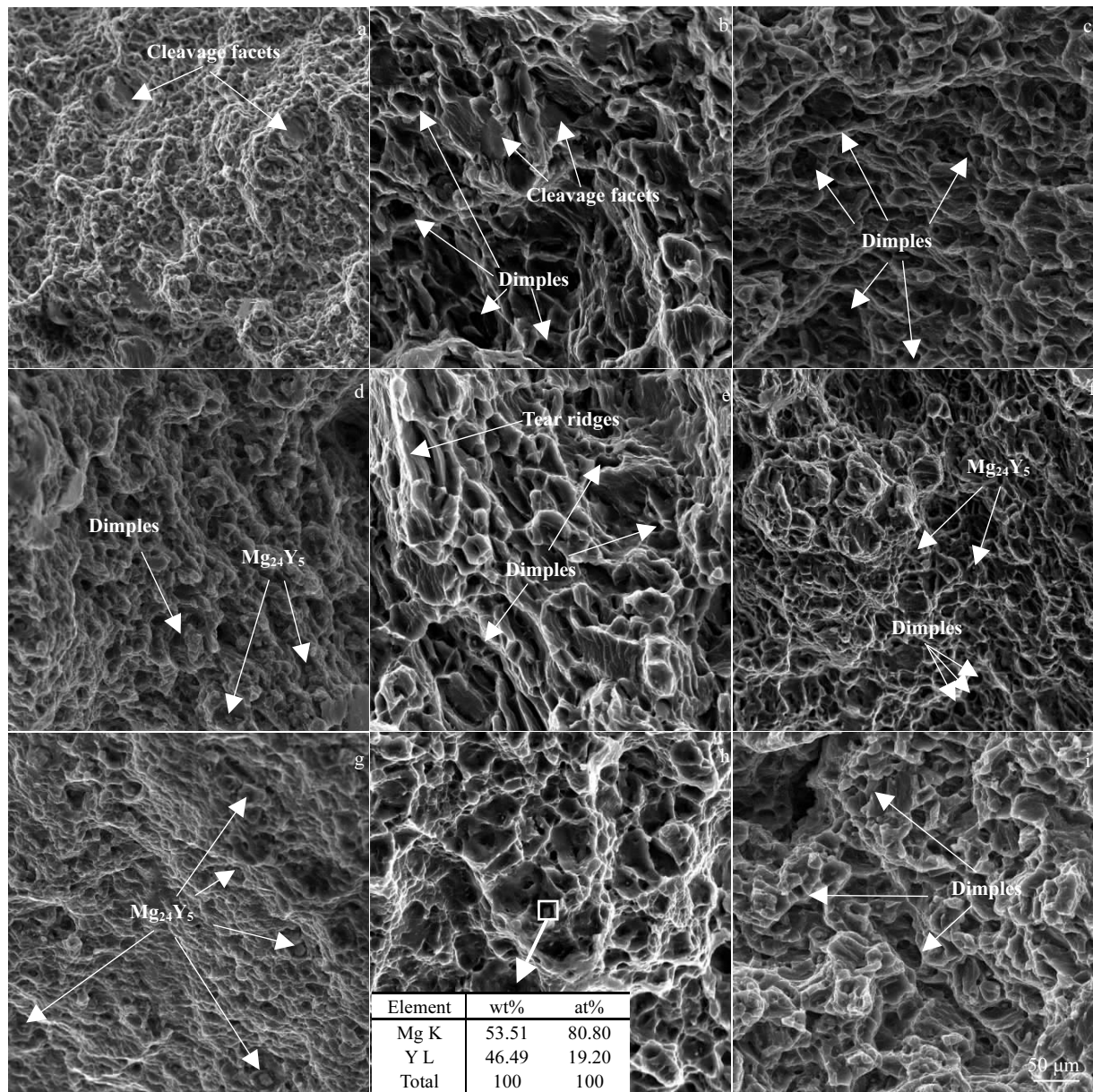


Fig.6 SEM images of fracture surfaces of the rolled and annealed: (a) as-rolled YKN0; (b) YKN0 annealed at 200 °C/1 h; (c) YKN0 annealed at 400 °C/20 min; (d) as-rolled YKN0.5; (e) YKN0.5 annealed at 200 °C/1 h; (f) YKN0.5 annealed at 400 °C/20 min; (g) as-rolled YKN1; (h) YKN1 annealed at 200 °C/1 h; (i) YKN1 annealed at 400 °C/20 min

where $\Delta\sigma_{GS}$ is the increase in yield stress due to grain refinement, K is the constant, and d is the average grain size. The constant K in Mg alloys can reach very high value (280~320 MPa· $\mu\text{m}^{-1/2}$)^[21]. Therefore, grain refinement strengthening plays an important role for the high strength of the wrought Mg-Y-Zr-xNd alloys. Secondly, the Mg₂₄Y₅ particles can act as strong pinning centers for grain boundaries and dislocations and then block the movement of dislocations. Hence, the improvement of mechanical properties is mainly due to the grain refinement and the formation of Mg₂₄Y₅ phases.

However, as shown in Table 2, the elongation slightly drops with the increase of Nd content. This may be due to the higher volume fraction of the Mg₂₄Y₅ phase particles in the alloys containing Nd (Fig.6h). Some of the fragile Mg₂₄Y₅ phase particles are not broken up during hot-rolled and may become the crack source during the tensile strength^[38], as indicated by the arrows in Fig.6. The elongation of alloys increases as the annealed temperature elevates, but with the addition of Nd optimal elongation of alloys appears at 200 °C/1 h. Clearly, the elongation of the annealed alloys is higher than that of as-rolled alloys. The excellent ductility of the annealed alloys sheets can be mainly ascribed to the following factors: (1) Grain refinement can be achieved by SRX, resulting in the higher deformation coordination capability. (2) The weakened basal texture facilitates activation of the sliding system.

Fig.6 show the SEM images of the tensile specimens of the as-rolled and subsequently annealed. As seen from Fig.6a, 6d and 6g, the fracture surface is composed of cleavage facets, tear ridges and dimples. The amount of tear ridges and dimples are consistent with the good elongation, while the cleavage planes are accompanied with brittle fracture. Therefore, quasi-cleavage fracture is the dominant fracture mechanism of the as-rolled Mg-Y-Zr-xNd alloys. With the increase of Nd content, the fracture of the alloy consists of more broken particles under the dimples, and the brittle fracture is more obvious. The fractured second phase is considered as Mg₂₄Y₅ according to EDS analysis (Fig.6h). Therefore, the decreased elongation with the increasing Nd addition may be attributed to the increase in the number of relatively large and fragile particles. A large number of dimples and a few tearing ridges appear was existent after annealing, indicating that ductile fracture is the main fracture mode of the annealed alloys. Since most Mg alloys have a hexagonal crystal structure and fewer slip systems, two or more slip systems are scarcely activated at the same time^[28]. However, the grain refinement caused by Nd addition and DRX and SRX can make the migration, slip and rotation of grain boundary easier. The crack direction changes frequently and the crack extension resistance increases during crack propagation, thereby tensile fracture changes from quasi-cleavage fracture to ductile fracture.

3 Conclusions

1) Minor Nd addition can effectively refine grains and

change phase compositions of Mg-Y-Zr alloy. The alloys with different Nd contents are mainly composed of α -Mg and Mg₂₄Y₅, and β (Mg₁₄Nd₂Y) phase appears when the Nd content is 1.01wt%. Nd content can decrease the solid solubility of Y atom in Mg and contribute to the formation of the Mg₂₄Y₅ phase.

2) The strength is enhanced with the increase of Nd content. As-rolled alloys containing 1.01wt%Nd exhibits maximum UTS and YS, and these values are 336 and 278 MPa, respectively. It is mainly due to the fine grains caused by DRX and SRX, and the dispersion distribution of high thermal stability of the Mg₂₄Y₅ and β phase which effectively prevent the dislocation movement and grain boundary slip.

3) The elongation decreases with the increase of Nd content and increases after annealing. The elongation of as-rolled YKN0 alloy is 18.5%, while that of the as-rolled YKN1 alloy is 16.3%. The elongation reduction with the increase of Nd addition may be explained by the increase in the number of relatively large and fragile particles. Grain refinement and weakening basal texture are the main reasons for the increase in elongation during annealing.

References

- 1 Wang X J, Xu D K, Wu R Z et al. *Journal of Materials Science & Technology*[J], 2018, 34(2): 245
- 2 Liu H, Huang H, Yang X et al. *Journal of Magnesium & Alloys*[J], 2017, 5(2): 231
- 3 Chen X H, Geng Y X, Pan F S. *Rare Metal Materials and Engineering*[J], 2016, 45(1): 13
- 4 Li Q, Huang G J, Huang X D et al. *Journal of Magnesium & Alloys*[J], 2017, 5(2): 166
- 5 Mordike B L, Ebert T. *Materials Science and Engineering A*[J], 2001, 302(1): 37
- 6 Kandalam S, Agrawal P, Avadhani G S. *Journal of Alloys and Compounds*[J], 2015, 623(25): 317
- 7 Alaneme K K, Okotete E A. *Journal of Magnesium & Alloys*[J], 2017, 5(4): 460
- 8 Kandalam S, Agrawal P, Avadhani G S et al. *Journal of Alloys and Compounds*[J], 2015, 623(25): 317
- 9 Mayama T, Ohashi T, Higashida K. *Materials Science Forum*[J], 2010, 654-656: 695
- 10 Fang X, Wu S, Zhao L et al. *Rare Metal Materials and Engineering*[J], 2016, 45(1): 7
- 11 Basu I, Al-Samman T. *Acta Materialia*[J], 2015, 96(1): 111
- 12 Li H, Öchsner A, Yarlalagadda P K D V et al. *Continuum Mechanics & Thermodynamics*[J], 2017(10): 1
- 13 Wu R Z, Qu Z K, Zhang M L. *Reviews on Advanced Materials Science*[J], 2010, 24(1): 35
- 14 Yang Z Z, Wang K, Fu P H et al. *Journal of Magnesium & Alloys*[J], 2018, 6(1): 44
- 15 Xin R, Song B, Zeng K et al. *Materials & Design*[J], 2012, 34: 384

- 16 Kekule T, Smola B, Vlach M et al. *Journal of Magnesium & Alloys*[J], 2017, 5(2): 173
- 17 Bettles C J, Gibson M A. *Advanced Engineering Materials*[J], 2010, 5(12): 859
- 18 Khomamizadeh F, Nami B, Khoshkhouei S. *Metallurgical and Materials Transactions A*[J], 2005, 36(12): 3489
- 19 Nie J F, Muddle B C. *Acta Materialia*[J], 2000, 48(8): 1691
- 20 Rokhlin L L. *Taylor and Francis*[J], 2003(10): 209
- 21 Wang X, Liu C, Xu L et al. *Journal of Materials Research*[J], 2013, 28(10): 1386
- 22 Li H, Lv F, Liang X et al. *Materials Science and Engineering A*[J], 2016, 667: 409
- 23 Xu X Y, Chen X H, Du W W et al. *Journal of Materials Science & Technology*[J], 2017, 33(9): 926
- 24 Hadorn J P, Hantzsche K, Yi S et al. *Metallurgical & Materials Transactions A*[J], 2012, 43(4): 1347
- 25 Kumar N, Choudhuri D, Banerjee R. *International Journal of Plasticity*[J], 2015, 68: 77
- 26 Zhang Q, Fan T W, Fu L et al. *Intermetallics*[J], 2012, 29(5): 21
- 27 Dou Y C. *Candidate for Doctorate*[D]. Chongqing: Chongqing University, 2015 (in Chinese)
- 28 Yu H Y, Yan H G, Chen J H et al. *Journal of Alloys and Compounds*[J], 2014, 586(4): 757
- 29 Robson J D, Henry D T, Davis B. *Acta Materialia*[J], 2009, 57(9): 2739
- 30 You S H, Huang Y D, Kainer K U et al. *Journal of Magnesium and Alloys*[J], 2017, 5(3): 239
- 31 Su J, Sanjari M, Kabir A S H et al. *Materials Science and Engineering A*[J], 2016, 662: 412
- 32 Chao H Y, Sun H F, Chen W Z et al. *Materials Characterization*[J], 2011, 62(3): 312
- 33 Nave M D, Barnett M R. *Scripta Materialia*[J], 2004, 51(9): 881
- 34 Engler O, Yang P, Kong X W. *Acta Materialia*[J], 1996, 44(8): 3349
- 35 Liu L Z, Chen X H, Pan F S. *Materials Science and Engineering A*[J], 2016, 669(4): 259
- 36 Jiang Y B, Guan L, Tang G Y. *Journal of Alloys & Compounds*[J], 2016, 656(25): 727
- 37 Bohlen J, Wendt J, Nienaber M et al. *Materials Characterization*[J], 2015, 101: 144
- 38 Ma C J, Liu M P, Wu G H et al. *Materials Science and Engineering A*[J], 2003, 349(1-2): 207

轧制及退火态的 Mg-Y-Zr-xNd 合金的组织 and 力学性能

代 言¹, 陈先华^{1,2}, 徐笑阳¹, 赵超越¹, 刘春全¹, 赵 娣¹,
刘 晓 芳¹, 罗 铸¹, 涂 腾¹, 潘 复 生^{1,2}

(1. 重庆大学 教育部轻合金国际联合实验室, 重庆 400044)

(2. 重庆市科学技术研究院, 重庆 401123)

摘 要: 通过 OM、SEM、XRD、EBSD 和拉伸试验研究了不同热处理条件下 Mg-5Y-0.6Zr-xNd ($x = 0, 0.5\%, 1\%$, 质量分数) 合金的组织 and 力学性能。结果表明, 随着 Nd 含量的增加, 第二相 $Mg_{24}Y_5$ 和 $Mg_{14}Nd_2Y$ (β) 在基体中的含量增加。添加少量 Nd 可以降低 α -Mg 的堆垛层错能, 促进热轧过程中的动态再结晶。随着 Nd 含量的增加, 静态再结晶的体积分数明显增加。退火处理后 Mg-5Y-0.6Zr-0Nd 合金的平均晶粒可细化至 $3.73 \mu m$ 。轧制合金的抗拉强度随着 Nd 的增加而增加, 而伸长率则表现出相反的变化趋势。含有 1.01%Nd 的轧制合金具有优良的机械性能, 其抗拉强度、屈服强度和伸长率分别为 336 MPa、278 MPa 和 16.3%。在微观结构观察的基础上, 讨论了力学性能的变化。

关键词: Mg-Y-Zr-Nd 合金; 组织; 力学性能; 再结晶

作者简介: 代 言, 男, 1995 年生, 硕士, 重庆大学材料科学与工程学院, 重庆 400045, 电话: 023-65102633, E-mail: yan.dai@cqu.edu.cn